Scheibbs, Austria

ESTIMATING CARBON STOCK IN UNMANAGED FORESTS USING FIELD DATA AND REMOTE SENSING

Thomas Leditznig

Abstract: Unmanaged forest ecosystems play a critical role in addressing the ongoing climate and biodiversity crises. A combination of RGB imagery from an Unmanned Aerial Vehicle (UAV), Sentinel-2 data and field surveys were used to determine the carbon stock of an unmanaged forest in the UNESCO World Heritage Site wilderness area Dürrenstein-Lassingtal. The approach demonstrated that the combination of low-cost remote sensing data and field work can predict above-ground biomass and carbon stock of unmanaged forests with high accuracy. The results and the estimation error distribution highlight the importance of accurate field data.

Keywords: Unmanned Aerial Vehicle, Sentinel-2, RGB imagery, machine learning, carbon storage capacity, unmanaged forests

BESTIMMUNG DES KOHLENSTOFFVORRATS IN UNBEWIRTSCHAFTETEN WÄLDERN MITTELS FELDDATEN UND FERNERKUNDUNG

Zusammenfassung: Unbewirtschaftete Waldökosysteme spielen eine entscheidende Rolle bei der Bewältigung der aktuellen Klima- und Biodiversitätskrise. In diesem Beitrag werden RGB-Aufnahmen einer Kamera-Drohne mit Sentinel-2-Daten und Feldstudien kombiniert. Das Ziel ist die Bestimmung des Kohlenstoffvorrats eines unbewirtschafteten Walds im UNESCO-Weltnaturerbe Wildnisgebiet Dürrenstein-Lassingtal. Durch die Kombination von kostengünstigen Fernerkundungsdaten und Felddaten konnte die oberirdische Biomasse und deren Kohlenstoffvorrat mit hoher Genauigkeit vorhergesagt werden. Die Ergebnisse und die Fehlerverteilung des Modells zeigen, dass die Qualität der Felddaten ausschlaggebend für die Genauigkeit der Modellierung ist.

Schlüsselwörter: Unmanned Aerial Vehicle, Sentinel-2, Orthophotos, Machine Learning, Kohlenstoffvorrat, unbewirtschaftete Wälder

1 INTRODUCTION

Unmanaged forests are critical for climate change mitigation and biodiversity conservation, but monitoring these mostly inaccessible areas requires cost-effective approaches (Luyssaert & Schulze et al. 2008). They are a refuge for endangered species and absorb significant amounts of carbon dioxide (CO_2) from the atmosphere (Paillet et al. 2010). The ongoing climate crisis, deforestation, and loss of biodiversity have increased the attention paid to these habitats. Recent investigations suggest that the carbon storage capacity of unmanaged near-natural forests has been underestimated for decades (Luyssaert et al. 2008). If protection and restoration measures were taken, global forests would have the potential to store additional 226 Gt of carbon in areas with low human influence (Mo et al. 2023). As this can only be achieved in intact ecosystems, these environments are becoming increasingly relevant for meeting global climate and biodiversity goals (Mo et al. 2023). Considering and monitoring the carbon storage capacity and the condition of old-growth and unmanaged forests becomes vital for understanding the influence of climate change on the carbon sequestration of woodlands (Chiti et al. 2024). As global warming will affect the carbon stock of forests in the next few years, the exact conditions of these habitats needs to be known (Luyssaert et al. 2008).

Author

Thomas Leditznig, BSc, MSc
Brandstatt 61
A-3270 Scheibbs
E: thomas.leditznig@outlook.com

Remote sensing is a potent alternative or at least a complement to traditional and costly forest inventories. As there is no commercial interest in most primary and unmanaged forests, an inventory method for assessing unmanaged forests needs to be budget friendly. New findings suggest that the combination of high-resolution RGB imagery, multispectral satellite imagery, Digital Surface Models (DSM) and supervised Machine Learning (ML) can be used to detect tree canopy cover and the Above Ground Biomass (AGB) with high accuracy (Iizuka et al. 2017). When combined with remote sensing techniques, in-situ measurements

DOI: 10.14627/gis.Science.2025.3.1

are only required for initial calibration and validation purposes when assessing woodlands (Lalechere et al. 2024). This principle also applies to carbon stock estimations derived from remote sensing data (Vicharnakorn et al. 2014). As there is hardly any detailed information on the condition and extent of unmanaged forests, the combination of sample field surveys and remote sensing techniques is a viable approach to monitor these habitats in a time- and cost-sensitive way (Fernandes 2020).

The main objective of this study is to propose a low-budget approach to approximate the carbon stock of unmanaged forests in remote locations using a combination of UAV RGB imagery, multispectral satellite imagery, and field data. In-situ measurements are used to determine the carbon storage capacity of the live tree biomass per square meter (m^2) and to assess the accuracy of the carbon storage approximation.

2 MATERIALS

2.1 STUDY AREA

The study area is located in the UNESCO World Heritage Site wilderness area Dürrenstein-Lassingtal in Austria. Situated in the province of Lower Austria, this protected site includes the largest remaining old-growth forest of the European Alps. Since 2003, the wilderness area is protected according to the IUCN standards Ia (strict nature reserve) and Ib (wilderness area) (Leroux et al. 2010). The study area is at the center of the wilderness area, covers roughly 5.76 ha and is protected by the standard IUCN Ib. It is surrounded by mountains and lies between 700 m and 750 m above sea level.

2.2 FIELD DATA

For the sample plots, circular plots with a size of 0.03 ha (planar) were defined (Inoue et al. 2014). Ten sample plots were randomly distributed across the defined woodland. Figure 1 shows the locations of the sample plots.

To document the parameters height (H), diameter at breast height (DBH), species and location for every tree, the software ArcGIS Field Maps (Environmental Systems Research Institute, Inc., Redlands, California) was used (Naik et al. 2021). Height values were derived using a Forestry Pro II laser ranger (Nikon Corporation, Tokyo, Japan), while the diameter at breast height was measured using a tree caliper at a stem height of 130 cm. Data from 511 trees with a $DBH > 1$ cm was captured.

2.3 REMOTE SENSING DATA

For the acquisition of the high-resolution RGB imagery, we used a DJI Mavic Mini (SZ DJI Technology Co., Shenzhen, China). Aerial images of the study area were acquired on August 4th, 2023.

A cloud free multispectral image of the study area was acquired from the Sentinel-2 L2A (Level 2A data) data catalog. The selected image was taken on August 13th, 2023, and displays no significant changes in land coverage compared to the drone flight on August 4th, as there were no extreme weather events in this period.

2.4 DATA ANALYSIS

For each sample plot, the live tree above-ground biomass was estimated based on the measured tree parameters. For most of the species found in the study area, the stem wood volume was determined using Denzin's standard formula (Eq. 1) (Denzin 1929). For the tree species European Spruce (Picea abies), Common Beech (Fagus sylvatica), and European Larch (Larix decidua), the improved formula (Eq. 2) described by Denzin (1929) was used.

$$V = \frac{DBH^2}{1000}. \tag{1}$$

$$V_{\text{improved}} = V + \left(V \cdot (H - H_{\text{normal}}) \cdot V_{\text{corr}}\right). \tag{2}$$

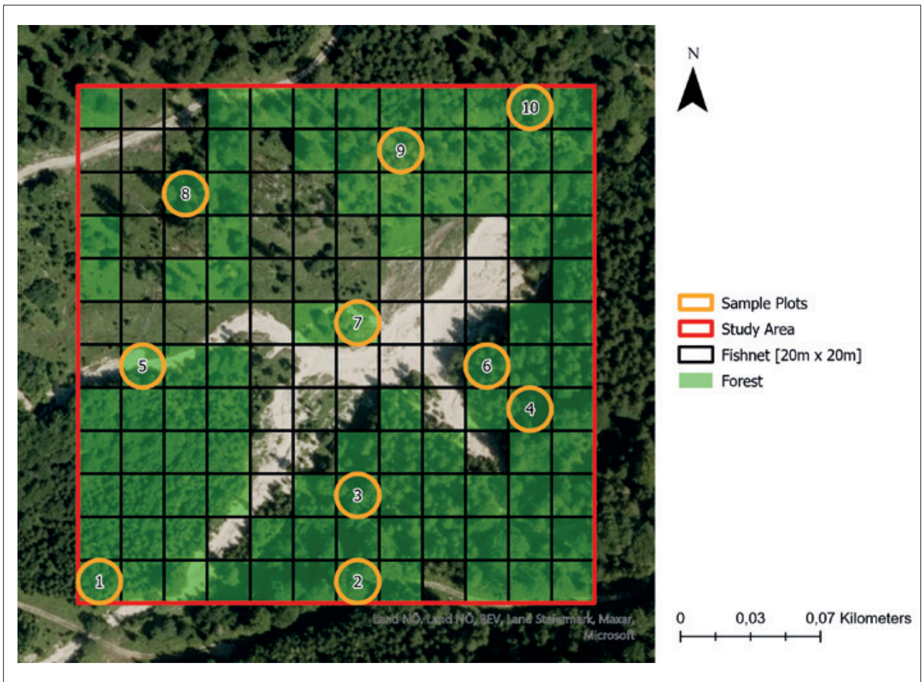

Figure 1: Sample plots for the in-situ measurements

To calculate carbon storage capacity, the different tree species were divided into two categories: coniferous and deciduous. The stem volume of each group was summarized for every individual field plot. To calculate the mass of the whole tree, including leaves, needles, branches and roots, the stem volume was multiplied with the average expansion ratio factor (Anderl et al. 2023). Based on the whole biomass of the tree, the corresponding carbon storage capacity was determined (Anderl et al. 2023). The conversion parameters are listed in Table 1.

The high-resolution RGB UAV images were processed using Agisoft Metashape (Agisoft LLC., St. Petersburg, Russia) in order to generate an orthomosaic and a DSM (Furukawa et al. 2021). The multispectral satellite images were used to calculate the Normalized Difference Vegetation Index

Conversion factor	Coniferous	Deciduous
m^3 to *t* dm (stemwood)	0.38	0.54
t dm stemwood to *t* dm whole tree	1.62	1.63
t dm to *t* C	0.50	0.48
t C to *t* CO_2	3.67	3.67
Summarized factor	1.13	1.55

Tabelle 1: *Conversion factors for the Austrian forest*

(NDVI) of the study area. The produced remote sensing datasets were combined to a multi-band composite raster dataset. The supervised machine learning algorithm Random Forest (RF) was used to classify the land cover of the generated composite in ArcGIS Pro (Environmental Systems Research Institute, Inc., Redlands, California) utilizing an object-based approach.

2.5 ACCURACY ASSESSMENT

The accuracy of the classification was tested with 100 random validation points per class and summarized in a Confusion Matrix (Anderl et al. 2023).

The accuracy of the carbon stock estimation was determined based on the in-situ measurements from the sample plots depicted in Figure 1. For each plot the approximated carbon storage capacity was compared to the measured storage capacity. Potential differences were quantified in absolute numbers, percentage values and standard error (SE).

3 RESULTS

3.1 ACQUIRED FIELD DATA

Roughly 85 % (434) of the 511 trees sampled were alive. Most of the trees found are European Spruce (56.7 %) and Common Beech (40.1 %). Other species sampled are European Larch, Common Ash (Fraxinus excelsior), Common Whitebeam (Sorbus aria), Common Hazel (Corylus avellana), Sycamore Maple (Acer pseudoplatanus), Wych Elm (Ulmus glabra) and Willow (Salix).

All field plots combined contain 65 054 m^3 of live tree AGB. With 49 544 m^3 (76.2 %), most of the biomass surveyed was coniferous wood. 15 511 m^3 (23.8 %) of the measured live tree biomass was categorized as deciduous wood. On average, a hectare of continuous forest (closed canopy forest) contains 313 421 ± 44 507 m^3 (mean ± standard error) of live tree biomass in the study area.

The carbon storage capacity of the forest area found in all field plots amounts to 80 016 t of CO_2. With 46 438 t of CO_2 (58.04 %), most of the carbon stock is located in the sample plots used for the approximation. In the study area, a hectare of woodland stores 371 423 ± 51 106 t of CO_2 on average.

3.2 LAND COVER CLASSIFICATION

The best performing classification algorithm, based on the datasets orthomosaic, NDVI and DSM, has a resolution of about 3.5 cm and covers the whole study area. Figure 2 depicts the generated raster dataset.

The classification of the study area achieved an overall accuracy (Total) of 80.8 % with a Kappa value of 0.743. The Confusion Matrix of the classification dataset is depicted in Table 2.

3.3 CARBON STOCK ESTIMATION

For the field plots, a total carbon storage capacity of 79 186 ± 10 896 t of CO_2 was estimated. The approximation of the carbon storage capacity of the field plots (based on the plots 1, 3,

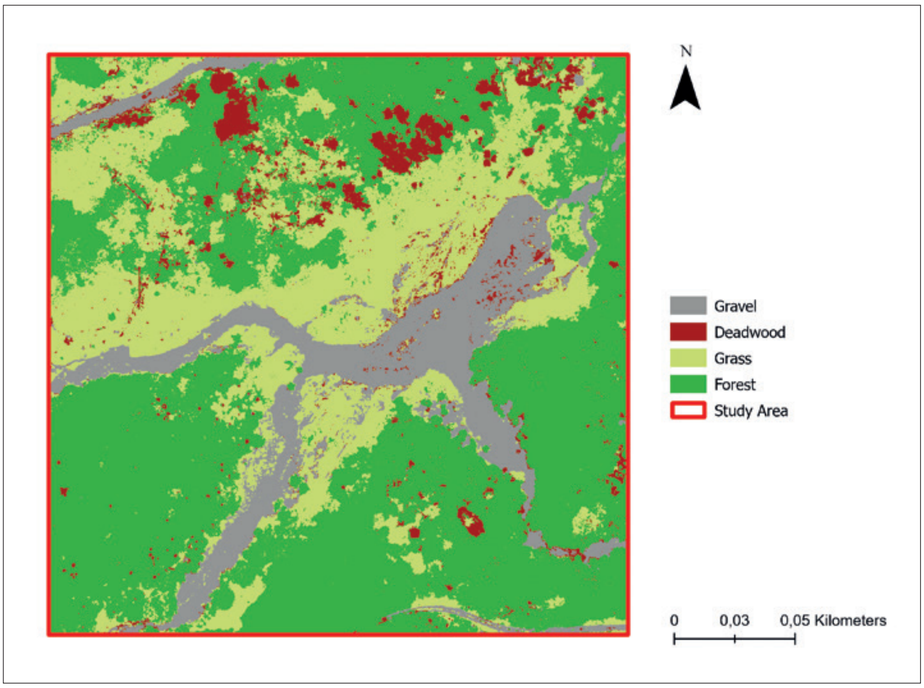

Figure 2: *Classification raster of the study area*

Class	Gravel	Deadw.	Grass	Forest	Total	U-Acc.	Kappa
Gravel	93	12	1	0	106	88 %	
Deadw.	6	81	0	2	89	91 %	
Grass	1	7	87	36	131	66 %	
Forest	0	0	12	62	74	84 %	
Total	100	100	100	100	400		
P-Acc.	93 %	81 %	87 %	62 %		80.8 %	
Kappa							0.74

Table 2: *Confusion Matrix of the classification dataset*

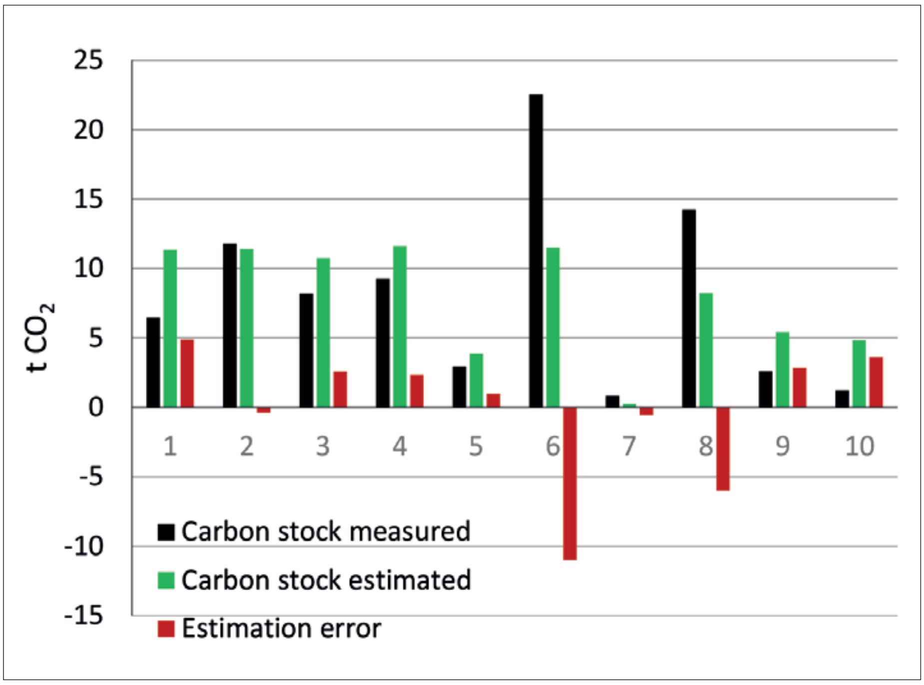

Figure 3: *Estimation error per plot*

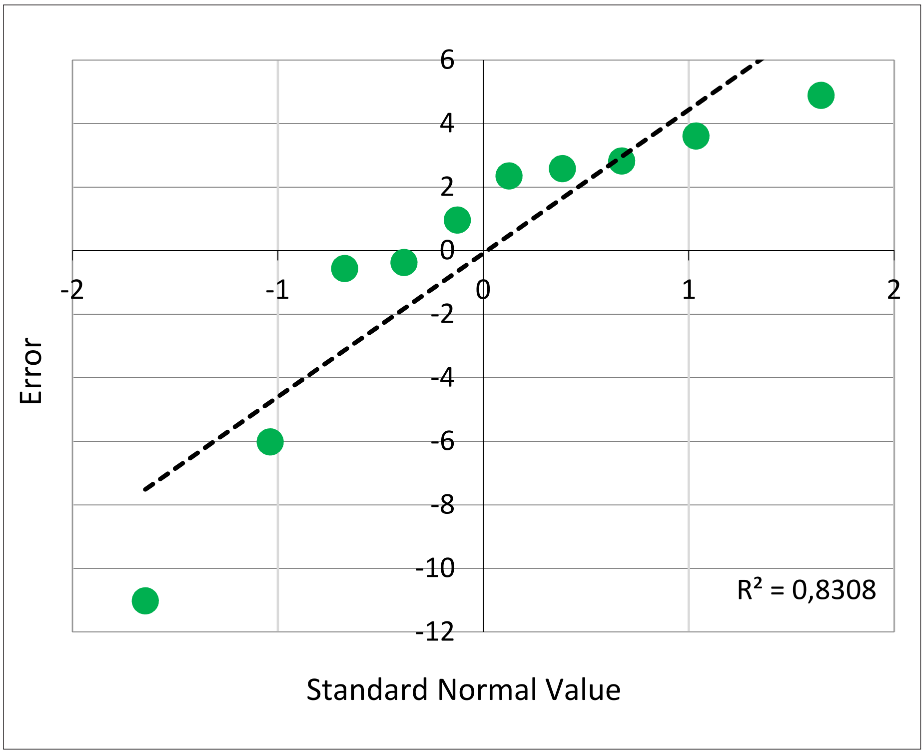

Figure 4: *Q-Q plot of the distribution of carbon stock estimation errors*

4 and 6) produced an overall error of −0.830 t of CO_2 (−1.0 %). The average error per plot is −0.083 t of CO_2, while the standard deviation of the errors amounts to ± 4648 t of CO_2 (± 5.9 %). Figure 3 depicts the estimation error per field plot.

With a median of 1652 t of CO_2 and a skewness of −1 285, the distribution of the errors is skewed to the left. The Pearson kurtosis indicates a peaked distribution with a value of 3543. Figure 4 is a Quantile-Quantile (Q-Q) plot of the distribution of the carbon stock estimation errors.

4 DISCUSSION

The structural properties of the researched forest area are like those of managed woodlands in Austria. This is not surprising, as the study area incorporates forests that were managed until 2001. Considering the altitude and the geomorphological structure of the study area, this estimation is also in line with the national average AGB for managed forests with 351 ± 3.3 m^3 per ha (Bundesministerium für Land- und Forstwirtschaft 2023). Based on the measured live tree biomass, the average carbon storage capacity per hectare amounts to 371 423 ± 51 106 t of CO_2. This value is in line with the methodology and the conclusions stated in Austria's Inventory Report 2023 (Anderl et al. 2023).

The near-natural forest studied is characterized by a high spatial variability. Topographic trends are affecting the structural properties of the forest. This indicates that the distribution of the sample plots has an impact on the estimation of the carbon storage capacity of the in-situ measurements. As field data is essential for the proposed approach, further investigation is necessary to improve the inventory and sampling design. A possible solution to improve the selection of sample plots for large-scale forest inventories could be to synthesize remote sensing data and machine learning technologies (Pohjankukka et al. 2022).

With an overall accuracy of 80.8 % and a Kappa value of 0.743, the composite consisting of the orthomosaic, NDVI, and DSM achieved the best result regarding the land cover classification. The results are comparable to those from Heuschmidt et al. (2020), who classified cork oak woodlands with an accuracy of 79.5 % using images captured by an UAV fitted with an RGB sensor. Natesan et al. (2019) also achieved 80 % classification accuracy with multitemporal airborne RGB images. Zhou et al. (2021) managed to score a higher overall accuracy with 90 % for the classification of different vegetation classes using RGB UAV imagery than the methodology described herein.

The classification generated in this study does not reach the scientifically accepted total accuracy threshold of 85 % and therefore cannot be recommended without further clarification (Anderson et al. 1976). As it can be very challenging to distinguish between the different types of vegetation without high-resolution multispectral imagery, this limit might be too harsh in some cases (Ayhan 2020). Foody (2008) points out, that this limit might be not applicable to all use cases. Ayhan (2020) suggests that an overall classification accuracy of about 78 % for a high-resolution RGB imagery segmentation should be viewed as sufficient. This interpretation is in line with the proposed findings.

With an overall error of about 1 %, the carbon storage capacity of the field plots was estimated accurately. The average error per plot for the carbon stock estimation is very low (–0.830 t of CO_2), while the calculated SE of ± 4648 t of CO_2 (5.9 %) can be described as substantial. The carbon stock estimation error varies significantly from plot to plot, which can be attributed to the structural parameters, e. g. sum of AGB and species composition, differing significantly across the study area. The findings of the in-situ measurements also show that the studied forest area is very heterogenous. The key figures median, skewness and Pearson kurtosis indicate that the estimation errors do not describe a perfect Gaussian distribution. Figure 4 verifies this assumption and implies that the error distribution only approximates a standard distribution and varies significantly with the structural parameters of the corresponding sample plot. Since the average carbon storage capacity is assigned to the broad vegetation class Forest per unit area (m^2), the estimated average value plays a critical role in the estimation.

5 CONCLUSION AND OUTLOOK

The study area in the wilderness area Dürrenstein-Lassingtal had similar AGB and carbon stock characteristics as a typical managed forest in Austria. With an overall accuracy of 80.8 %, the land cover classification based on a composite consisting of high-resolution RGB imagery, DSM and NDVI values proves to be a reliable basis for carbon stock estimation.

Combining field data, UAV derived datasets and Sentinel-2 satellite imagery proved to be an efficient option for estimating the carbon stock of unmanaged forests. The combined carbon storage capacity of the surveyed field plots was underestimated by 1 %. Due to the high variability of carbon stock found in the study area, the SE of the estimated storage capacity of ± 10896 t of CO_2 (± 13.6 %) and the SE of the overall estimation error of ± 4648 t of CO_2 (± 5.8 %) provide a better understanding of the accuracy that can be achieved by the proposed approach.

Future work should focus on the classification of different woodland types and tree species of unmanaged forests. A distinction between coniferous and deciduous trees, as applied in Austria's National Inventory Report (Anderl et al. 2023), would allow for a carbon stock analysis based on the specific carbon storage capacities of the different wood categories. A multitemporal approach, such as the methodology proposed by Grybas & Congalton (2021), may allow to accurately detect tree species with consumer-grade UAVs. Current progress in the field of UAV technology improves the availability of high-resolution multispectral imagery via new platforms like the DJI Mavic 3(M) Multispectral (DJI 2023) and allows for more in-depth land cover assessments (Fonseka et al. 2024).

References

Anderl, M.; Colson, J.; Gangl, M. et al. (2023): Austria's National Inventory Report 2023. Submission under the United Nations Framework Convention on Climate Change.

Anderson, J. R.; Hardy, E. E.; Roach, J. T.; Witmer, R. E. (1976): A Land Use and Land Cover Classification System for Use with Remote Sensor Data. Geological Survey Professional, Paper 964.

Ayhan, B.; Kwan, C. (2020): Tree, Shrub, and Grass Classification Using Only RGB Images. In: Remote Sensing 12 (8), 1333.

Bundesministerium für Land- und Forstwirtschaft, Klima- und Umweltschutz, Regionen und Wasserwirtschaft (2023): Datensammlung zum Österreichischen Wald. https://info.bml.gv.at/themen/wald/wald-in-oesterreich/wald-und-zahlen/waldbericht/datensammlung-zum-oesterrreichischen-wald.html (16. 07. 2025).

Chiti, T.; Benilli, N.; Mastrolonardo, G.; Certini, G. (2024): The potential for an old-growth forest to store carbon in the topsoil: A case study at Sasso Fratino, Italy. In: Journal of Forestry Research 35 (1).

Denzin, A. (1929): Schätzung der Masse stehender Waldbäume. In: Forstarchiv 5, pp. 382 – 384.

DJI (2023): DJI Mavic 3M. https://ag.dji.com/de/mavic-3-m (16. 07. 2025).

Fernandes, M. R.; Aguiar, F. C.; Martins, M. J. et al. (2020): Carbon Stock Estimations in a Mediterranean Riparian Forest: A Case Study Combining Field Data and UAV Imagery. In: Forests 11 (4), 376.

Fonseka, C. L. I. S.; Halloluwa, T.; Hewagamage, K. P. et al. (2024): A dataset of unmanned aerial vehicle multispectral images acquired over a field to identify nitrogen requirements. In: Data in Brief 110479.

Foody, G. M. (2008): Harshness in image classification accuracy assessment. In: International Journal of Remote Sensing 29 (11), pp. 3137 – 3158.

Furukawa, F.; Laneng, L. A.; Ando, H. et al. (2021): Comparison of RGB and Multispectral Unmanned Aerial Vehicle for Monitoring Vegetation Coverage Changes on a Landslide Area. In: Drones 5 (3), 97.

Grybas, H.; Congalton, R. (2021): A Comparison of Multi-Temporal RGB and Multispectral UAS Imagery for Tree Species Classification in Heterogeneous New Hampshire Forests. In: Remote Sensing 13 (13), 2631.

Heuschmidt, F.; Gómez-Candón, D.; Soares, C. et al. (2020): Cork oak woodland land-cover types classification: a comparison between UAV sensed imagery and field survey. In: International Journal of Remote Sensing 41 (19), pp. 7649 – 7659.

Iizuka, K.; Yonehara, T.; Itoh, M.; Kosugi, Y. (2017): Estimating Tree Height and Diameter at Breast Height (DBH) from Digital Surface Models and Orthophotos Obtained with an Unmanned Aerial System for a Japanese Cypress (Chamaecyparis obtusa) Forest. In: Remote Sensing 10 (2), 13.

Inoue, T.; Nagai, S.; Yamashita, S. et al. (2014): Unmanned Aerial Survey of Fallen Trees in a Deciduous Broadleaved Forest in Eastern Japan. In: PLoS ONE 9 (10), e109881.

Lalechere, E.; Monnet, J. M.; Breen, J.; Fuhr, M. (2024): Assessing the potential of remote sensing-based models to predict old-growth forests on large spatiotemporal scales. In: Journal of Environmental Management 351, 119865.

Leroux, S. J.; Krawchuk, M. A.; Schmiegelow, F. et al. (2010): Global protected areas and IUCN designations: Do the categories match the conditions? In: Biological Conservation 143 (3), pp. 609 – 616.

Luyssaert, S.; Schulze, E. D.; Börner, A. et al. (2008): Old-growth forests as global carbon sinks. In: Nature 455 (7210), pp. 213 – 215.

Mo, L.; Zohner, C. M.; Reich, P. B. et al. (2023): Integrated global assessment of the natural forest carbon potential. In: Nature 624 (7990), pp. 92 – 101.

Naik, P.; Dalponte, M.; Bruzzone, L. (2021): Prediction of Forest Aboveground Biomass Using Multitemporal Multispectral Remote Sensing Data. In: Remote Sensing 13 (7), 1282.

Natesan, S.; Armenakis, C.; Vepakomma, U. (2019): Resnet-based Tree Species Classification Using UAV Images. In: The International Archives of the Photogrammetry, Remote Sensing and Spatial Information Sciences XLII-2/W13, pp. 475 – 481.

Paillet, Y.; Bergès, L.; Hjältén, J. et al. (2010): Biodiversity Differences between Managed and Unmanaged Forests: Meta-Analysis of Species Richness in Europe. In: Conservation Biology 24 (1), pp. 101 – 112.

Pohjankukka, J.; Tuominen, S.; Heikkonen, J. (2022): Bayesian Approach for Optimizing Forest Inventory Survey Sampling with Remote Sensing Data. In: Forests 13 (10), 1692.

Vicharnakorn, P.; Shrestha, R.; Nagai, M. et al. (2014): Carbon Stock Assessment Using Remote Sensing and Forest Inventory Data in Savannakhet, Lao PDR. In: Remote Sensing 6 (6), pp. 5452 – 5479.

Zhou, R.; Yang, C.; Li, E. et al. (2021): Object-Based Wetland Vegetation Classification Using Multi-Feature Selection of Unoccupied Aerial Vehicle RGB Imagery. In: Remote Sensing 13 (23), 4910.